

# Radii in the $sd$ shell and the $s_{1/2}$ “halo” orbit: A game changer

J. Bonnard<sup>1</sup> and A. P. Zuker<sup>2,3</sup>

<sup>1</sup> *Istituto Nazionale di Fisica Nucleare, Sezione di Padova, 35131 Padova, Italy*

<sup>2</sup> *Dipartimento di Fisica e Astronomia, Università degli Studi di Padova, I-35131 Padova, Italy*

<sup>3</sup> *Université de Strasbourg, IPHC, CNRS, UMR7178, 23 rue du Loess 67037 Strasbourg, France*

(Dated: June 13, 2016)

Proton radii of nuclei in the  $sd$  shell depart appreciably from the asymptotic law,  $\rho_\pi = \rho_0 A^{1/3}$ . The departure exhibits systematic trends fairly well described by a single phenomenological term in the Duflo-Zuker formulation, which also happens to explain the sudden increase in slope in the isotope shifts of several chains at neutron number  $N = 28$ . It was recently shown that this term is associated with the abnormally large size of the  $s_{1/2}$  and  $p$  orbits in the  $sd$  and  $pf$  shells respectively. Further to explore the problem, we propose to calculate microscopically radii in the former. Since the (square) radius is basically a one body operator, its evolution is dictated by single particle occupancies determined by shell model calculations. Assuming that the departure from the asymptotic form is entirely due to the  $s_{1/2}$  orbit, the expectation value  $\langle s_{1/2} | r^2 | s_{1/2} \rangle$  is determined by demanding that its evolution be such as to describe well nuclear radii. It does, for an orbit that remains very large (about 1.6 fm bigger than its  $d$  counterparts) up to  $N, Z = 14$  then drops abruptly but remains some 0.6 fm larger than the  $d$  orbits. An unexpected behavior bound to challenge our understanding of shell formation.

As selfbound systems, nuclei have volumes that go as the number of particles  $A$ . Therefore their radii go as  $A^{1/3}$ . As both neutrons and protons are present, an isospin dependence is also expected. Duflo and Zuker (DZ) [1] proposed the following ( $t = N - Z$ )

$$\sqrt{\langle r_\pi^2 \rangle} = \rho_\pi = A^{1/3} \left( \rho - \frac{\zeta}{2} \frac{t}{A^{4/3}} - \frac{v}{2} \left( \frac{t}{A} \right)^2 \right) e^{(g/A)} (1)$$

$$+ \lambda [z(D_\pi - z)/D_\pi^2 \times n(D_\nu - n)/D_\nu^2] A^{-1/3} \quad (2)$$

where the exponential term accounts for the larger size of light nuclei,  $v$  measures the overall dilation or contraction as a function of  $t^2$ , and  $\zeta$  is responsible for the difference in radii between the fluids *i.e.*, the neutron skin

$$\Delta r_{\nu\pi} = \rho_\nu - \rho_\pi = \zeta t e^{g/A} / A.$$

In Eq. (2)  $n, z$  are the number of active particles between the extruder-intruder (EI) magic numbers [2, Sec. IC] at  $N, Z = 6, 14, 28, 50 \dots$ ;  $D_x = 8, 14, 22 \dots$  are the corresponding degeneracies. We shall use two data sets:

TABLE I. Results of fits through Eqs.(1) and (1)+(2) including  $\nu$  data points with  $Z \leq Z_M$  and  $N \geq Z$  from data sets D [3] and AM [4] with fixed  $\zeta = 0.8$  fm.  $\rho, g, \lambda, v$ , root mean square deviations (rmsd) in fm.

$\rho$	$g$	$\lambda$	$v$	Data	$\nu$	$Z_M$	rmsd
0.946	1.422	0.000	0.550	D	636	96	0.0299
0.942	1.513	0.000	0.312	AM	876	96	0.0365
0.950	1.232	0.000	0.312	D	88	30	0.0415
0.947	1.370	0.000	0.295	AM	107	30	0.0419
0.942	0.948	6.857	0.526	D	636	96	0.0132
0.940	0.879	7.719	0.297	AM	876	96	0.0203
0.944	0.985	5.562	0.368	D	88	30	0.0176
0.940	1.140	5.208	0.334	AM	107	30	0.0246

D; The original Duflo compilation (unpublished, available on request) in which the extraction of  $\rho_\pi$  from iso-

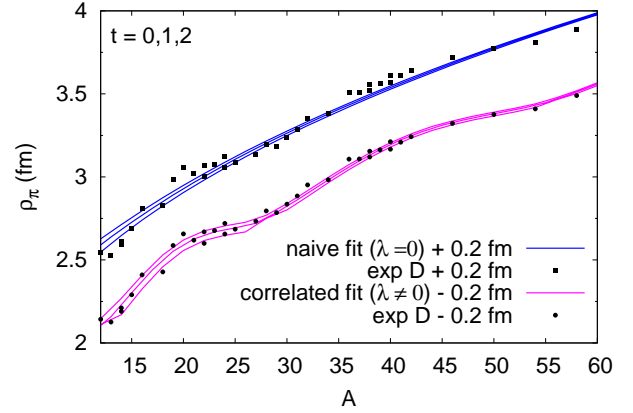


FIG. 1. (color online) Illustrating the influence of the  $\lambda$  term. Duflo (D) fits for  $t = 0, 1, 2$  and  $Z \leq 30$  with  $\lambda = 0$  and  $\lambda \neq 0$  (labelled naive and correlated respectively).

tope shifts  $\delta r^2$  was examined in detail [3]. The set used in DZ [1].

AM; The recent Angeli-Marinova compilation [4].

The quality of the fits depends little on the  $\zeta$  coefficient in the range  $0.4 < \zeta < 1.2$  fm. The chosen value  $\zeta = 0.8$  fm corresponds to the DZ estimate for the neutron skin  $\Delta r_{\nu\pi}$ . It is seen from Table I that the inclusion of  $\lambda$  (the Duflo term from now on) in the fit makes an enormous difference. We know from reference [5] that it makes it possible to explain the—hitherto puzzling—increase of slope in the Ca and K isotope shifts. In Figure 1 it is seen that for the  $sd$  and  $pf$  shells the indifferent results of the naive fit ( $\lambda = 0$ , rmsd = 0.0415 fm) evolve into truly satisfactory patterns for the correlated values,  $\lambda = 5.562$  fm, rmsd = 0.0176 fm. In general Table I makes it clear that its beneficial effects extends to all regions.

To obtain a microscopic description of the mechanisms

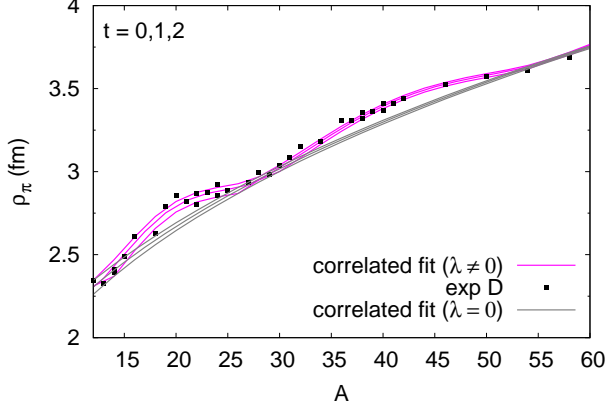


FIG. 2. (color online) As Fig. 1 with the naive fit ( $\lambda = 0$ ) replaced by the result of using the parameters of the correlated fit setting  $\lambda = 0$ .

involved we start by adapting [6, Eq.(2.157)]

$$\langle r_\pi^2 \rangle = \frac{41.47}{\hbar\omega_\pi} \sum_i m_i (p_i + 3/2 + \delta_i)/A, \quad (3)$$

where  $m_i$  and  $p_i$  stand for the total occupancy and principal quantum number of the orbit  $i$ , and  $\delta_i$  denotes the necessary correction to the harmonic oscillator value  $\langle i|r^2|i \rangle = p_i + 3/2$  to describe the observed radii. In principle protons and neutrons must be treated separately but we know that  $\langle r_\pi^2 \rangle$  must be close to  $\langle r_\nu^2 \rangle$ , depend on neutron occupancies (as made evident by the form of Eq.(2)) and be insensitive to  $\zeta$ . The way out is to adopt an isospin representation *i.e.*, sum over  $A$  rather than  $Z$  and allow for isospin dependence through Eq. (1). To enforce Eq. (3) it is necessary to separate the average trend from the fluctuations we want to calculate. This is achieved in Figure 2 where the former is defined by the parameters of the full fit but setting  $\lambda = 0$ , which defines a baseline for each  $t$ . The—now definite positive—fluctuations lie above it. We know that the origin of the Duflo term, Eq. (2) must be found in the halo orbits. Concentrating on the  $sd$  shell, the  $s_{1/2}$  orbit is taken to be solely responsible for the fluctuations. Setting  $\delta_i = 0$  for  $i = d_{5/2,3/2}$  and  $\delta_i = \delta$  for  $s_{1/2}$ , Eq.(3) becomes:

$$\langle r_\pi^2 \rangle = \rho_\pi(\lambda = 0) + \frac{41.47}{\hbar\omega} \frac{m_{s_{1/2}} \delta}{A}. \quad (4)$$

It remains to extract the occupancies  $m_{s_{1/2}}$  from shell model calculations. The overall saturation properties are treated in the usual fashion: The two-body matrix elements are taken to scale as  $W(\hbar\omega) = W(\hbar\omega_0)\hbar\omega/\hbar\omega_0$ , where the oscillator frequency is obtained through [6, Eq.(2.157)]

$$\hbar\omega = \frac{41.47}{\langle r_\pi^2 \rangle} \sum_i z_i (p_i + 3/2)/Z. \quad (5)$$

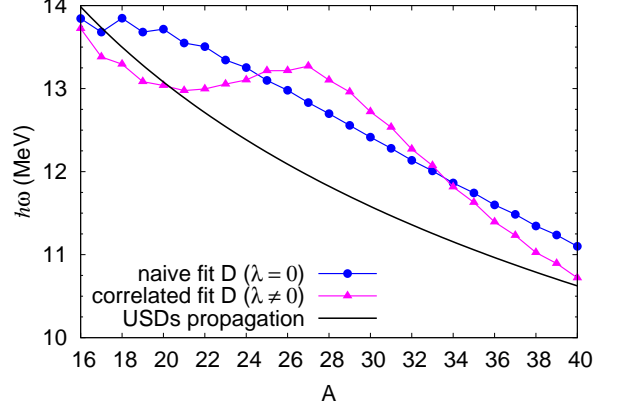


FIG. 3. (color online) Evolution of  $\hbar\omega$  for naive, correlated and USD assumptions [7]. Only  $t = 0$  and 1 cases are included, merged in a single curve which leads to the slight observed staggering. See text after (5).

The form of  $\hbar\omega$  as a function of  $A$  ensues from a term by term (nucleus by nucleus) evaluation of Eq. (5). In Figure 3 three possibilities are examined. The naive and correlated curves follow from radii obtained with Eqs. (1) and (1)+(2) respectively. The USDs form  $\hbar\omega = \hbar\omega(A=18)(18/A)^{0.3}$ , consistent with the crudest  $\rho_\pi = \rho_0 A^{1/3}$  law is also shown. Calculations will be done with the USDa interaction [8] and a monopole corrected interaction (MCI) propagated according to the correlated pattern in Figure 3. Its specifications will be given at the end. Now we return to Eq. (4), define  $\hbar\omega$  through the

TABLE II. Results for the optimal  $\delta$ 's for D and AM sets of data, and for the USDa and MCI interactions for  $t = 0, 1$  and 2. The rmsd are calculated with respect to all known radii in the  $sd$  shell (21 and 23 for D and AM respectively).

	Duflo		Angeli-Marinova	
	USDa	MCI	USDa	MCI
$\delta_<$	4.90	4.25	5.50	4.80
$\delta_>$	1.40	1.35	1.45	1.35
rmsd (fm)	0.023	0.020	0.023	0.018

correlated fit with  $\lambda = 0$ , assume  $\delta_i = 0$  for  $i = d_{5/2,3/2}$  and  $\delta_i = \delta$  for  $s_{1/2}$ . The favored solutions have the form

$$\delta = \begin{cases} \delta_< & \text{if } N \text{ and } Z < 14 \\ \delta_> & \text{if } N \text{ or } Z \geq 14. \end{cases} \quad (6)$$

A search for the optimal parameters yields the values in Table II leading to Figures 4 in which the microscopically calculated radii are compared with the phenomenological ones obtained with the Duflo term. It appears that the microscopic results reproduce the observed radii at least as well as the phenomenological fit for the D set, and much better in the AM case. The rmsd for MCI is smaller than for USDa, and so are the calculated sizes of the  $s_{1/2}$

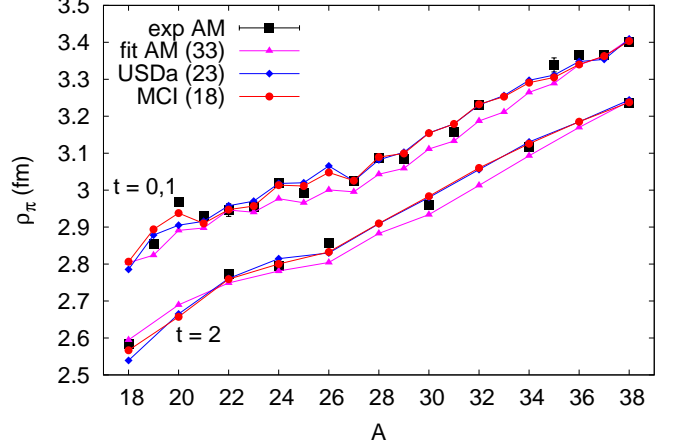
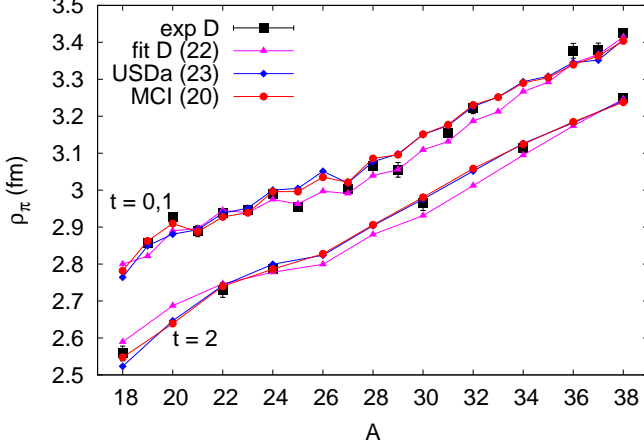


FIG. 4. (color online) Illustrating the solution of Eq. (3). Behavior of  $\rho_\pi$  for USDa and MCI calculations for data sets D and AM compared with the phenomenological fit. The  $t = 0$  and 1 cases are conflated in a single curve. These and  $t = 2$  values are shifted by  $\pm 0.07$  fm, respectively, for clarity. In parenthesis the rmsd for the different cases in millifemtometers (see Table II).

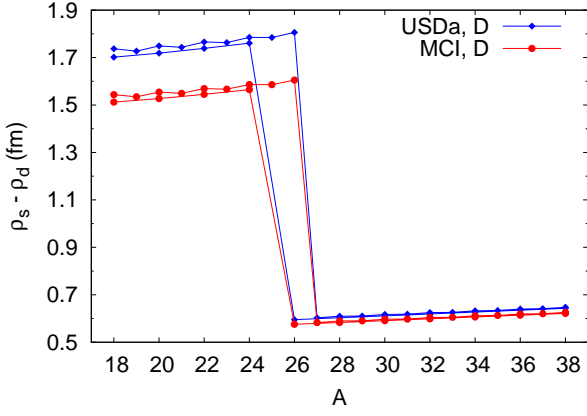


FIG. 5. (color online) Differences in root mean square radii  $\rho_s - \rho_d = \sqrt{\langle r_{s1/2}^2 \rangle} - \sqrt{\langle r_d^2 \rangle}$  from Eq. (4). The mean differences (in fm) associated to the upper and lower  $\delta$  values in Table II are (1.56, 0.6) for MCI D, (1.75, 0.62) for USDa D (both included in the plot); and (1.76, 0.6) for MCI AM, (1.93, 0.69) for USD AM (not shown in the plot).

orbit shown in Figure 5. The quantitative differences between cases fade next to the striking pattern revealed by the figure, which raises a hard—open—question:

Can the behavior of the  $s_{1/2}$  halo orbit seen in the figure be derived from *ab initio* calculations with existing interactions?

The reader is invited to judge whether this question is genuine or merely rhetorical. Here we offer some points of reference. The halo orbits are the essential ingredient in halo nuclei [9, 10]. What we are finding is that they have a pervasive influence throughout. Their description will most likely require non local potentials [11, 12]. At present only relativistic mean-field calculations seem capable of reproducing the slope increase in isotope shifts (as in [13] using interaction DD-ME2 [14]).

Let us explore next what can be learned by comparing the USDa and MCI interactions that have proved quite helpful so far. The specification of MCI that follows is included for completeness. The reader may choose to jump to the comments following Figure 6.

The monopole corrected interaction MCI [15]—part of the no-core project outlined in [5]—is derived from the N3LO potential [16] through a  $V_{\text{low-}k}$  regularization [17] with cutoff  $\Lambda = 2 \text{ fm}^{-1}$  at  $\hbar\omega = 14 \text{ MeV}$ . Renormalization amounts to an overall 1.1 multiplicative factor and a 30% boost of the quadrupole force [18] plus the monopole corrections defined below. The whole is scaled as  $\text{MCI}(\hbar\omega) = \text{MCI}(14)\mathcal{P}$  with  $\mathcal{P} = \hbar\omega/14$ , where  $\hbar\omega$  follows the correlated form in Figure 3.

The monopole corrections are given in terms of operators in the “invariant representation” [19] in which the one- and two-body number operators  $m_t$  and  $m_t m_u$  are separated into a term that contains only the total number operator  $m$ , single-particle terms  $\Gamma_t^{(1)}$ , and two-body terms  $\Gamma_{tu}^{(1)}$ :

$$m_t \equiv m + \Gamma_t^{(1)}, \quad (7)$$

$$\frac{m_t(m_u - \delta_{tu})}{1 + \delta_{tu}} \equiv \frac{1}{2}m^{(2)} + (m-1)\Gamma_t^{(1)} + \Gamma_{tu}^{(2)}. \quad (8)$$

For our purpose it is convenient to associate each orbit  $t$  with its complement  $ct$  containing all orbits in the space except  $t$ . The degeneracy of  $t$  is  $D_t = 2(2j_t + 1)$  and that of its complement  $D_{ct} = D - D_t$ ,  $D$  being the total degeneracy of the valence space. In the  $sd$  shell, orbits  $d_{5/2}$ ,  $s_{1/2}$  and  $d_{3/2}$  will be called 5, 1, 3 respectively. The complement of 5, say, is  $c5 = 1 + 3$ . With this convention:

$$\Gamma_t^{(1)} = \frac{m_t D_{ct} - m_{ct} D_t}{D}, \quad (9)$$

$$\Gamma_t^{(2)} = \left( \frac{m_t^{(2)}}{D_t^{(2)}} + \frac{m_{ct}^{(2)}}{D_{ct}^{(2)}} - \frac{2m_t m_{ct}}{D_t D_{ct}} \right) \frac{D_t^{(2)} D_{ct}^{(2)}}{(D_t + D_{ct})^{(2)}} \quad (10)$$

Under particle-hole transformations  $m_t \rightarrow \bar{m}_t = D_t - m_t$ ,  $\Gamma_t^{(1)}$  changes sign and  $\Gamma_t^{(2)}$  is invariant.

The monopole corrections take the form

$$V_{MC} = e_5 \Gamma_5^{(1)}(m-1) + 0.06 \Gamma_1^{(1)}(m-1) + \quad (11)$$

$$2.0 \Gamma_3^{(1)}(m-1)(\bar{m}-1)/(D/2-1)^2 + \quad (12)$$

$$(1.0 \Gamma_5^{(2)} + 0.5 \Gamma_3^{(2)})(\bar{m})\mathcal{P}/D, \quad (13)$$

where  $e_5 = -0.05$  if  $A \leq 28$ ;  $e_5 = -0.11$  if  $A > 28$ . All coefficients in MeV. The sum of Equations (11)+(12) defines propagated single-particle operators  $\eta_t$  such that  $\sum_t \eta_t D_t = 0$ , shown in Fig. 6. Note that the sum (12)+(13) amounts to a three body contribution because of the factors  $\bar{m}-1$  in (12) and  $\bar{m}$  in (13).

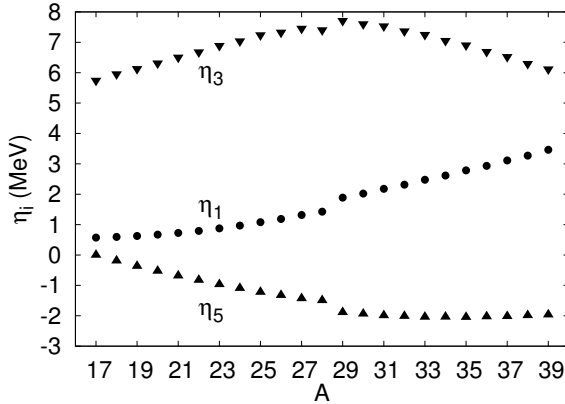


FIG. 6. The propagated single-particle energies  $\eta_i$  from Eqs. (11) and (12)

The discontinuity in Figure 6 responds to a sudden

rmsd raise in the spectra after  $N, Z = 14$ : An embarrassing puzzle when the MCI was derived turned out to be a premonitory signal of the discontinuity in Figure 5.

While USDa is an open multiparametric fit, MCI tends to assign to each term a definite function. Both reflect the influence of the halo orbit. Explicitly in the case of MCI, implicitly for USDa: The significant reduction in rmsd—from about 280 keV in MCI to some 140 keV in USDa, for a total of 196 states with  $t = 0, 1$  and  $2$ —is due to relatively minor and hitherto unexplained differences in matrix elements, which now must be unambiguously attributed to the  $s_{1/2}$  halo orbit. Note that for purely yrast states the MCI rmsd are close to those of USDa.

To conclude, let us address the heart of the matter: A crucial unsolved problem in nuclear physics is the origin of the observed EI closures. Spectroscopically it is associated with the difficulty of having the correct  $J = 3$  spin for the ground state of  $^{10}\text{B}$  with potentially exact calculations using two-body forces [20]: The smoking gun in favor of three body forces. The problem persists for the ground state of  $^{22}\text{Na}$  and a possible solution has been proposed [21, section 7] involving terms such as  $\Gamma_5^{(2)}$  in (13) which ensures that  $^{22}\text{O}$  is a good closed shell and  $^{22}\text{Na}$  has the correct ground state spin: Useful phenomenology whose hidden foundations leave open the problem of shell formation.

But then: where are the halo orbits in all this? Could it not be that EI closures are not associated to selfbinding of the orbits of largest  $j$  in a major oscillator shell—due to three-body forces—but to unbinding of the halo orbits above them?

It sounds improbable, but as Sherlock Holmes put it *Once you eliminate the impossible, whatever remains, no matter how improbable, must be the truth.*

- 
- [1] J. Duflo and A. P. Zuker, Phys. Rev. C **66**, 051304 (2002).
  - [2] E. Caurier, G. Martínez-Pinedo, F. Nowacki, A. Poves, and A. P. Zuker, Rev. Mod. Phys. **77**, 427 (2005).
  - [3] J. Duflo, Nuclear Physics A **576**, 29 (1994).
  - [4] I. Angeli and K. Marinova, Atomic Data and Nuclear Data Tables **99**, 69 (2013).
  - [5] J. Bonnard, S. M. Lenzi, and A. P. Zuker, Phys. Rev. Lett. **116**, 212501 (2016).
  - [6] A. Bohr and B. R. Mottelson, *Nuclear Structure, vol. I* (Benjamin, New York, 1969).
  - [7] B. A. Brown and B. H. Wildenthal, Annu. Rev. Nucl. Part. Sci. **38**, 29 (1988).
  - [8] B. A. Brown and W. A. Richter, Phys. Rev. C **74**, 034315 (2006).
  - [9] I. Tanihata, H. Savajols, and R. Kanungo, Progress in Particle and Nuclear Physics **68**, 215 (2013).
  - [10] T. Frederico, A. Delfino, L. Tomio, and M. Yamashita, Progress in Particle and Nuclear Physics **67**, 939 (2012).
  - [11] F. Perey and B. Buck, Nuclear Physics **32**, 353 (1962).
  - [12] G. H. Rawitscher, Nuclear Physics A **886**, 1 (2012).
  - [13] K. Kreim, M. Bissell, J. Papuga, K. Blaum, M. D. Rydt, R. G. Ruiz, S. Goriely, H. Heylen, M. Kowalska, R. Neugart, G. Neyens, W. Nrtershuser, M. Rajabali, R. S. Alarcn, H. Stroke, and D. Yordanov, Physics Letters B **731**, 97 (2014).
  - [14] G. A. Lalazissis, T. Nikšić, D. Vretenar, and P. Ring, Phys. Rev. C **71**, 024312 (2005).
  - [15] A. P. Zuker, “Monopole corrected interactions,” unpublished (2016).
  - [16] D. R. Entem and R. Machleidt, Phys. Lett. B **524**, 93 (2002).
  - [17] S. Bogner, T. Kuo, and A. Schwenk, Physics Reports **386**, 1 (2003).
  - [18] M. Dufour and A. P. Zuker, Phys. Rev. C **54**, 1641 (1996).
  - [19] A. Abzouzi, E. Caurier, and A. P. Zuker, Phys. Rev. Lett. **66**, 1134 (1991).
  - [20] P. Navrátil and W. E. Ormand, Phys. Rev. Lett. **88**, 152502 (2002).
  - [21] J. Mendoza-Temis, J. G. Hirsch, and A. P. Zuker, Nuclear Physics A **843**, 14 (2010).